

Technical Notes

TECHNICAL NOTES are short manuscripts describing new developments or important results of a preliminary nature. These Notes cannot exceed 6 manuscript pages and 3 figures; a page of text may be substituted for a figure and vice versa. After informal review by the editors, they may be published within a few months of the date of receipt. Style requirements are the same as for regular contributions (see inside back cover).

Analyzing Mistuning of Bladed Disks by Symmetry and Reduced-Order Aerodynamic Modeling

B. Shapiro*

University of Maryland, College Park, Maryland 20852

and

K. E. Willcox†

Massachusetts Institute of Technology,
Cambridge, Massachusetts 02139

Introduction

THE mistuned behavior of bladed disks is analyzed and optimized using an unsteady, transonic, computational fluid dynamic model (CFD). This result is enabled by the integration of two frameworks: the first is based on symmetry arguments and an eigenvalue/vector perturbation scheme, while the second is a model reduction technique based on the proper orthogonal decomposition (POD). The first framework reduces the complexity of the mistuning problem, reveals engineering tradeoffs and suggests the existence of an intentional robust mistuning which improves both stability and forced response with respect to random variations in blade parameters. The second framework permits the reduction of state-of-the-art computational fluid dynamic codes to reduced-order models, which capture the accuracy of the original simulation but still fit within the mistuning analysis framework. Together, these methodologies allow the analysis of a transonic, bladed disk with stiffness mistuning (see Fig. 1). Moreover, because of the low order of the aeroelastic model, a robust control μ uncertainty analysis can be used to prove that the intentional mistuning suggested by the symmetry analysis framework is indeed robust. Hence this paper contains the first rigorous demonstration that intentional mistuning can robustly improve both the stability and forced response for a model that includes sophisticated aerodynamic effects.

Mistuning Analysis Framework

The mistuning analysis framework used in this paper is developed in detail by Shapiro.^{1,2} The approach is based on symmetry arguments and an eigenvalue/eigenvector perturbation scheme which holds for any mistuning model (be it linear, nonlinear, of high or low dimensionality) and provides constraints on all aspects of the problem (from initial model formulation through intermediate analysis up to the final robust optimization problem).

Received 10 September 2001; revision received 13 May 2002; accepted for publication 27 August 2002. Copyright © 2002 by B. Shapiro and K. E. Willcox. Published by the American Institute of Aeronautics and Astronautics, Inc., with permission. Copies of this paper may be made for personal or internal use, on condition that the copier pay the \$10.00 per-copy fee to the Copyright Clearance Center, Inc., 222 Rosewood Drive, Danvers, MA 01923; include the code 0748-4658/03 \$10.00 in correspondence with the CCC.

*Assistant Professor, Aerospace Engineering; benshap@eng.umd.edu.

†Assistant Professor, Department of Aeronautics and Astronautics; kwillcox@mit.edu.

Linear Problem: Stability and Forced Response

From a practical point of view, we are concerned primarily with small blade deformations and so any nonlinear model reduces to the standard linear problem

$$\dot{x} = M(z)x + B_\ell(z)e^{i\ell\Omega t} \quad (1)$$

where $x = (x_1, x_2, \dots, x_r) \in \mathbb{R}^m$ is the state vector with $x_i \in \mathbb{R}^m$ corresponding to aerodynamic and structural states for the i th blade. Here r is the number of blades, m is the states per blade. Mistuning is represented by the vector $z \in \mathbb{R}^r$: an element $z_i \in \mathbb{R}$ denotes mistuning for the i th blade. Thus $M(z)$ is the linearization of the unfurced dynamics and B_ℓ is the forcing vector corresponding to the ℓ th spatial forcing mode: $d(\theta) = \sin(\ell\theta)$.

Equation (1) describes both stability and forced response. Stability deals with the mistuned eigenvalues $\lambda(z)$ of $M(z)$ and describes the change in damping or flutter boundaries with mistuning. Once stability is established, forced response is written as

$$X(z) = [i\omega I - M(z)]^{-1} B_\ell(z) \quad (2)$$

in the frequency domain. Since forced response essentially determines high cycle fatigue or blade life, it is crucial to understand how response X depends on mistuning z .

Eigenvalue/Vector Perturbation Under Symmetry

Both eigenvalues λ and response X have symmetries.² Eigenvalues are invariant under a mistuning rotation $\lambda(z) = \lambda(\varphi z)$, where φ is an operator that rotates vectors of size r to the left. Similarly, the response X has symmetry $\varphi X(z) = p_\ell X(\varphi z)$ where $p_\ell = \exp[2\pi i \ell / r]$. This implies that if we know the first blade dynamics $X_1(z)$ for all mistuning z , then we know the response for all other blades by symmetry.

It follows from the symmetry $\lambda(z) = \lambda(\varphi z)$ that the mistuned eigenvalues have expansion

$$\lambda(z) = \lambda(0) + a \sum_{i=1}^r z_i + z^T S z + \mathcal{O}(\|z\|^3) \quad (3)$$

where a is a complex scalar and S is a complex symmetric circulant matrix that is fully described by $r/2 + 1$ complex coefficients.

In order to find an approximation for the forced response $X(z)$, we represent the inverse matrix $A^{-1}(z) = [i\omega I - M(z)]^{-1}$ in Eq. (2) in terms of its mistuned eigenvalues $\mu(z) = 1/[i\omega - \lambda(z)]$ and left, right eigenvectors $U(z)$, $V(z)$ of $M(z)$. Notice that $\lambda(z)$ can be close to $i\omega$ when the eigenvalues are lightly damped and forced near resonance. By perturbing $\lambda(z)$ up to second order in the denominator of $\mu(z)$, as in Eq. (3), we can get an accurate approximation for $\mu(z)$ that captures the steep nonlinear dependence on mistuning. Together with a linear approximation of the eigenvectors $U(z)$, $V(z)$, we can calculate how the spatial forcing vector $B_\ell(z)$ projects onto the mistuned mode shapes. This yields a linear approximation for the numerator of $X(z) = A^{-1}(z) B_\ell(z)$ and, together with the quadratic approximation of $\mu(z)$ in the denominator, provides a complete description. Specifically, the response of blade one is given by

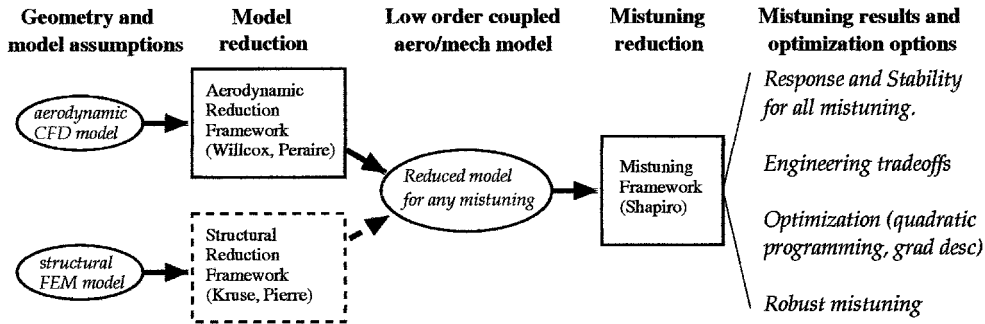


Fig. 1 Combination of tools for mistuning analysis. (The ----, box is not employed in the current paper; instead, a simple mass/spring structural model was used.)

$$X_1(z) = \sum_{j=0}^{r-1} \sum_{d=1}^m X_1^{j,d}(z) \approx \sum_{j=0}^{r-1} \sum_{d=1}^m \frac{\alpha_0^{j,d} + \alpha_1^{j,d} z_1 + \alpha_2^{j,d} z_2 + \cdots + \alpha_r^{j,d} z_r}{i\omega - \lambda_j^d(0) - a_{j,d} \sum_{i=1}^r z_i - z^T [S_{j,d}] z} \quad (4)$$

and the response of all other blades is described by symmetry. Here, all the coefficients in (4) are model dependent and superscripts denote indexing (not powers).

Reduced-Order Aerodynamic Modeling Framework

We require an aerodynamic model of the form (1) with a sufficiently low number of states per blade so that it is practical to perform the mistuning analysis above. Simplified-physics and assumed-frequency models are widely used, but have limitations, especially in the mistuning context. Hence we need a way of developing reduced-order, high-fidelity models that are valid over a range of frequencies and damping. This can be achieved via reduced-order modeling in which the CFD method is projected onto a small, carefully chosen, set of basis vectors. Our framework for developing these reduced-order models is outlined fully in Willcox.³

The model order reduction process used here is general and can be applied to a wide variety of CFD models. However, we consider a finite volume formulation of the linearized unsteady two-dimensional Euler equations (inviscid, compressible flow) on an unstructured grid as a specific case. This CFD formulation is described fully in Willcox,³ along with validation against experimental data for steady and unsteady turbomachinery flows.

The reduced-order model is obtained by projecting the CFD model onto a set of efficient basis vectors. The POD^{4,5} has been widely used in the field of fluid dynamics to compute an efficient orthonormal basis.⁶ Here, an efficient frequency domain version of the POD is used⁷⁻⁹ to generate a set of instantaneous flow solutions or snapshots at an appropriate set of spatial and temporal frequencies, which are characteristic of the flow problems under consideration. These snapshots are then used to compute the basis vectors via the POD process. The perturbation solution is then projected onto a small number of these basis functions and, using orthogonality, a system of ordinary differential equations for the modal coefficients is obtained. Along with transformations from interblade phase angle to blade coordinates,¹⁰ the final set of aerodynamic equations is obtained as

$$\dot{v} = Av + Bu + E_\ell d \quad (5)$$

$$y = Cv + Du + F_\ell d \quad (6)$$

where matrices A , B , C and D are block circular, $v \in \mathbb{R}^{rp}$ is the aerodynamic state with p POD modes per blade, $u \in \mathbb{R}^{rq}$ describes the instantaneous blade deflection with q deflection states per blade and $y \in \mathbb{R}^{rs}$ are the aerodynamic forces with s forces per blade. Finally, d captures the amplitude of the time-varying ℓ th spatial mode disturbance—such as an ℓ th mode time-varying pressure or velocity distortion at the inlet.

Coupling with a Mistuned Structural Model

In the above, the blade motion inputs u are specified and the system (5), (6) is time-marched to determine the resulting aerodynamic response. For a coupled analysis, equations of motion describing the structural states must be included in the reduced-order model. We consider here a simple mass-spring-damper structural model where each blade can move in plunging motion with a natural frequency of ω_h . Allowing mistuning in the blade stiffness, and further non-dimensionalizing time by $t' = kMt$ so that the blade tuned natural frequency is unity, the structural equations of motion for blade j with mass m and chord c can be written as

$$\ddot{h}_j + 2(1 + z_j)\zeta \dot{h}_j + (1 + z_j)^2 h_j = -(2/\pi \mu k^2) C_l^j \quad (7)$$

where $C_l^j = y_j$ is the lift coefficient for blade j , ζ is the structural damping, $k = \omega_h c / V$ is the reduced frequency and $\mu = 4m/\pi \rho c^2$, is the blade mass ratio. Here V is the steady-state inlet flow velocity, while M is the steady-state inlet Mach number. Note that because of the assumed form of the damping term in (7), a single parameter z_j is used to capture the mistuning effect on the stiffness and the damping.

The structural system (7) can be rewritten as a first order system for each blade j

$$\dot{u}_j = S(z_j)u_j + Ty_j \quad (8)$$

and coupled with the aerodynamic model (5), (6) to obtain dynamics for blade 1,

$$\begin{bmatrix} \dot{v}_1 \\ \dot{u}_1 \end{bmatrix} = \begin{bmatrix} \overbrace{A_1 \quad B_1}^{M_1(z_1)} \\ TC_1 \quad S(z_1) + TD_1 \end{bmatrix} \begin{bmatrix} v_1 \\ u_1 \end{bmatrix} + \begin{bmatrix} \overbrace{A_2 \quad B_2}^{M_2} \\ TC_2 \quad TD_2 \end{bmatrix} \begin{bmatrix} v_2 \\ u_2 \end{bmatrix} + \cdots + \begin{bmatrix} \overbrace{A_r \quad B_r}^{M_r} \\ TC_r \quad TD_r \end{bmatrix} \begin{bmatrix} v_r \\ u_r \end{bmatrix} + \underbrace{\begin{bmatrix} E_1 \\ TF_1 \end{bmatrix}}_{\beta_\ell} e^{i\omega t} \quad (9)$$

If we let $x_j = [v_j, u_j]$ and note that the dynamics for all other blades follow from symmetry, then we get a complete system which is a special case of Eq. (1).

Results for a Transonic Bladed Disk Model

The case chosen to demonstrate the framework is the DFVLR transonic cascade, analyzed with 20 blades at a steady-state inlet flow Mach number of $M = 0.82$ and a relative flow angle of 58.5 deg. The reduced-order aerodynamic model has six POD modes per blade. This aerodynamic model is coupled with a simple mass/spring structural system which models plunging motion only (and thus has two states per blade), and includes stiffness mistuning. Hence the final aeroelastic model has $(6 + 2) \times 20 = 160$ states.

Throughout the remainder of this section we will focus on three cases. Here, $\eta = \max_j Re[\lambda_j(0)]$ denotes the minimum tuned damping of the coupled aero/mechanical system.

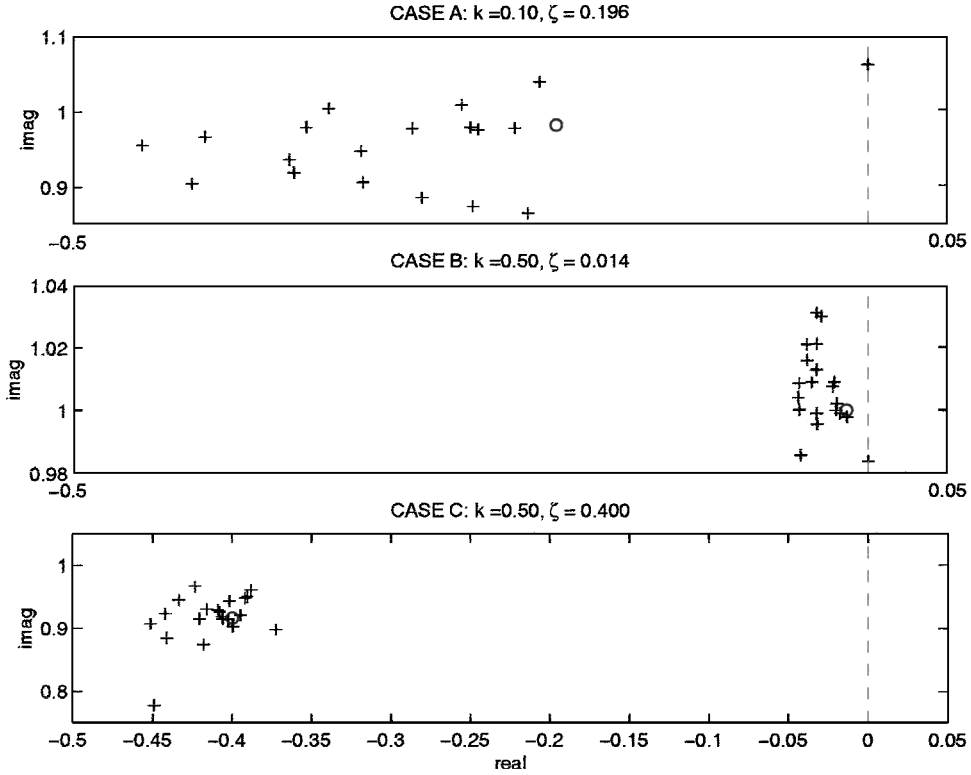


Fig. 2 Tuned system eigenvalues for cases A, B, and C. Eigenvalues shown (+) originate from the blade-alone structural mode (O) at $[-\zeta, \sqrt{(1 - \zeta^2)}]$.

Case A: High blade coupling, low system damping:

$$k = 0.10, \quad \eta = -0.33 \times 10^{-4}$$

Case B: Low blade coupling, low system damping:

$$k = 0.50, \quad \eta = -0.33 \times 10^{-4}$$

Case C: Low blade coupling, high system damping:

$$k = 0.50, \quad \eta = -1.23 \times 10^{-1}$$

Figure 2 shows the tuned eigenvalues for these three cases. It can be seen from the figure that in cases A and B, the parameters have been chosen so that the tuned system is barely stable. Case A has eigenvalues near and far from the imaginary axis and will have a very high forced response sensitivity. Case B has nearby eigenvalues which will veer sharply with mistuning. Case C will also exhibit sharp veering, but since all the eigenvalues are significantly damped this will cause neither a stability nor forced response sensitivity.

Sensitivity of Flutter Boundaries to Mistuning

The transition to flutter occurs when a system eigenvalue first crosses into the right half plane. For the model under consideration, there are three parameters which control this eigenvalue motion. They are 1) the reduced frequency k , decreasing k is destabilizing, 2) the structural damping ζ , decreasing ζ is destabilizing, and 3) the mistuning z which can be stabilizing or destabilizing. When mistuning shifts the least stable eigenvalue/s to the left, it delays the onset of flutter with respect to k and ζ .

Consequently, flutter boundary sensitivity to mistuning is determined by how fast the least stable eigenvalues move as a function of mistuning. Recall from Eq. (3) that eigenvalues move quadratically with zero average mistuning (the linear averaged part simply corresponds to a tuned parameter change). Hence the appropriate measure of eigenvalue speed along the real axis is $\|Re(S_j)\|/|Re(a_j)|$ which measures the quadratic mistuned dependence versus the linear tuned motion. Metric $\|Re(S_j)\|/|Re(a_j)|$ was computed for

Table 1 All mistuning directions stabilizing (+), all destabilizing (-), neither (\pm)

Mistuning sensitivity of:	Metric	Case A	Case B	Case C
Eigenvalue motion	$\pm \ Re(S_j)\ / Re(a_j) $	+116.9	+607.1	-1.107

Table 2 Worst case forced response sensitivity averaged over (200) random mistuning vectors with zero mean and 2% variance

Mistuning sensitivity of:	Metric	Case A	Case B	Case C
Forced response	$\ X(z_{md})\ / X(0) $	6.7	1.8	1.038

the least stable eigenvalue in cases A, B and C. To differentiate between stabilizing and destabilizing mistunings; the metric is given a positive sign if all mistuning vectors are stabilizing, a negative sign if all mistuning vectors are destabilizing, and both signs when there exist stabilizing and destabilizing mistuning vectors.

The results in Table 1 are as expected; eigenvalue motion is fastest in case B which has nearby tuned eigenvalues and eigenvalue motion is slowest in case C where the least stable mode is aerodynamic (does not originate from the blade-alone structural eigenvalue) and is essentially independent of mistuning. It is important to note that the metric above only deals with initial eigenvalue motion, it says nothing about eigenvalue motion for large z .

Sensitivity of Forced Response to Mistuning

In this section we compare the forced response sensitivity of cases A, B and C. First, we pick an external disturbance spatial mode $\ell = 11$ which corresponds to 11 stationary struts upstream. Second, we pick a set of 200 small random mistuning vectors \hat{z}^j , $j = 1, 2, \dots, 200$, where each blade mistuning value is chosen from a normal distribution with zero mean and 2% variance. Now for cases A, B and C we define $\|X(z)\| = \max_{(w,j)} |X_j(z, w)|$ where

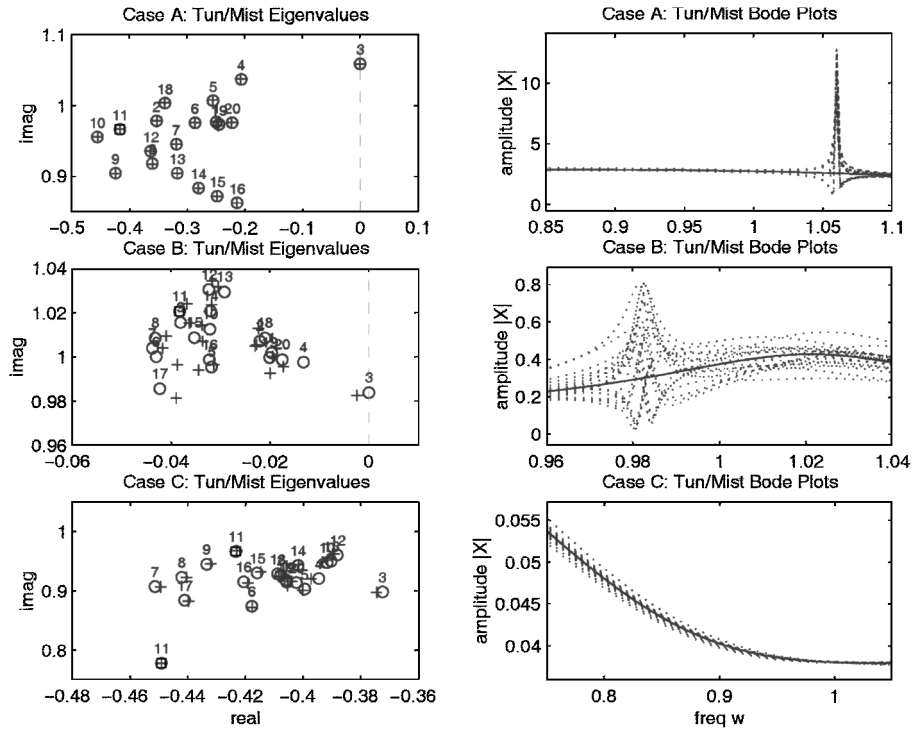


Fig. 3 Left side: O, tuned eigenvalues numbered by their nodal diameter. The $\ell = 11$ spatial forcing mode only excites the (boxed) 11th nodal diameter eigenvalues. +, mistuned eigenvalues for the same small random mistuning in all three cases. Now the $\ell = 11$ forcing excites all of the modes. Right side: Amplitude of tuned forced response vs frequency is denoted by the —, curve; because all blades have equal amplitude, there is only one curve. Mistuned forced response amplitudes for all 20 blades are shown by \dots , curves. The resonance caused by the third nodal diameter eigenvalue can be clearly seen in cases A and B. (Note the difference in axis scales for the three cases.)

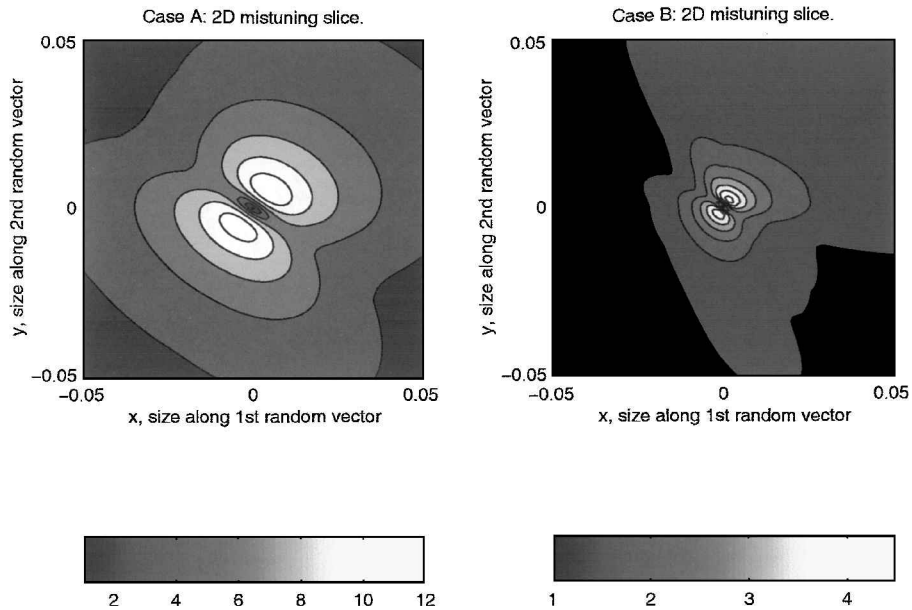


Fig. 4 Two-dimensional slice of the 20-dimensional mistuning space for cases A and B. Mistuning at each point (x, y) is given by $z = xz_1 + yz_2$, where z_1 and z_2 are zero-average mistuning vectors randomly chosen from a normal distribution with mean = 0 and variance = 1. The color at each point shows the (exact) worst-case mistuned response normalized by the worst-case tuned response: $\|X(z)\|/\|X(0)\|$. All points shown are stable. [Compare this figure with the schematic of Fig. 12 in,² and with Table 2. Note the difference in scales between cases A and B.]

$|X_j(z, w)|$ is the (exact) vibration amplitude of blade j at frequency w and mistuning z . Hence $\|X(z)\|$ is the worst-case single blade vibration amplitude over all forcing frequencies. Using this we compute the forced response sensitivity metric $\|X(z_{md})\|/\|X(0)\|$ where the overbar denotes an average over the 200 mistuning vectors. The corresponding results are listed in Table 2.

Even though it is cases B and C (with their nearby tuned eigenvalues) that exhibit the most severe eigenvalue veering, it is clear that case A has the most sensitive forced response. Figure 3 explains this behavior. This figure shows the mistuned behavior for

a small representative random mistuning $z = z_{md}$. The left side of the figure shows the tuned (O) versus mistuned (+) eigenvalues. In all three cases, the eigenvalue motion is small. Since the outside forcing is in the 11th spatial mode ($\ell = 11$), only the 11th modes are excited in the tuned case (the corresponding eigenvalues are boxed in Fig. 3). Once mistuning appears, the 11th spatial mode forcing excites all modes including the lightly damped 3rd mode. The difference in damping between mode 11 and mode 3 is most pronounced in case A and this explains the high forced response sensitivity. This resonance at mode 3 can be clearly seen in both

Table 3 Summary of mistuning behavior for transonic model

Behavior type	Mistuning metric or condition	Case A	Case B	Case C
Eigenvalue motion	$\pm \ Re(S_j)\ / Re(a_j) $	+116.9	+607.1	-1.107
Forced response	$\ X(\hat{z})\ /\ X(0)\ , \hat{z}_i \in N(0, 0.02)^a$	6.7	1.8	1.038
Prob unacceptable response	$P(\ X(\hat{z})\ > 5\ X(0)\ , \hat{z}_i \in U[\pm 0.01])^b$	85%	7%	0%
Robust mistuning?	$\ X(z^* + \hat{z})\ < 5\ X(0)\ , \forall \hat{z}_i \leq 0.01$	✓	✓	—

^aOverbar denotes average, $N(\text{mean}, \text{var})$ means a normal distribution.

^b $U(\pm\delta)$ denotes a uniform distribution from $-\delta$ to δ . For more detailed descriptions see previous section.

case A (at frequency $w = 1.06$) and case B (at frequency $w = 0.98$). In case B, the forced response behavior is complicated further by the presence of other nearby eigenvalues. Case C exhibits eigenvalue veering, but since all modes are significantly damped this does not cause a forced response sensitivity.

Figure 4 shows a two-dimensional slice through the 20-dimensional mistuning space. The color of the plot shows the size of the (worst case) forced response at each mistuning value for a mode $\ell = 11$ outside spatial forcing. In both cases A and B, there is a small region about the origin where the worst-case forced response is small. This is surrounded by an area of high worst-case forced response. Beyond this is a region where the worst-case forced response is small once again. This generic behavior was predicted by Shapiro² (in particular, compare Fig. 4 with Fig. 12 of Shapiro²).

Intentional Robust Optimal Mistuning

Figure 4 suggests that we can robustly improve worst-case forced response if we introduce a mistuning that moves the least damped (here 3rd nodal diameter) eigenvalue sufficiently far to the left. Effectively, we need an intentional mistuning that is sufficiently large to jump across the high worst-cased forced response region in Fig. 4. Then we know that small variations about this intentional mistuning (as caused by manufacturing uncertainty) will still keep the least damped eigenvalue relatively far inside the left-half plane (because eigenvalues move smoothly with parameters) and so our resonant response will remain acceptable.

To find the optimal mistuning that pushes the least stable eigenvalue left as effectively as possible, we can solve a quadratic programming optimization problem: minimize $s(z) = z^T Re[S_{j,d}]z$ subject to $|z_i| \leq \epsilon$ and $\sum_i z_i = 0$. We can find global optima for this problem by using a branch and bound method.¹¹ In both cases A and B, the optimal solution is in the ‘first’ mode $z^* = (\epsilon, \epsilon, \dots, \epsilon, -\epsilon, -\epsilon, \dots, -\epsilon)$. The advantage of our optimization problem phrased above is that it is globally tractable and it improves both flutter boundaries and forced response. The disadvantage is that it is based on an approximate problem and applies only when the behavior is dominated by a single eigenvalue (as is the case here).

We now check the robustness of our optimal solution on the exact (no mistuning approximation) model. Suppose in both cases A and B it is determined that a worst-case mistuned response of $\|X(\hat{z})\| > 5\|X(0)\|$ is unacceptable. For a 1% random mistuning (\hat{z}_i uniformly distributed between -0.01 and 0.01) there is a 85% probability in case A, and a 7% probability in case B, that the worst-case forced response will be above this level (based on a Monte Carlo simulation of the exact model). Hence the tuned point is not robust to small mistuning perturbations. Now let $\epsilon = 0.1$ and introduce the intentional optimal mistuning $z^* = \epsilon(1, 1, \dots, 1, -1, -1, \dots, -1)$. By a μ structured uncertainty robust performance analysis,¹² we have proved that $\|X(z^* + \hat{z})\| < 5\|X(0)\|$ for all $|\hat{z}_i| \leq 0.01$ in cases A and B. Hence we have shown (on the exact model) that for all mistuning near the optimal ($z = z^* + \hat{z}, |\hat{z}_i| \leq 0.01$) the system is stable and the forced response remains acceptable, i.e. we have proved rigorously that there is a 0% probability of either instability or unacceptable forced response at the intentionally mistuned point.

The associated results for the three parameter cases chosen are outlined in Table 3. Neither cases A nor B are robust at the origin. Even a small 1% variation in mistuning can lead to unacceptable

forced response. In both cases A and B it is possible to introduce the robust optimal ‘first mode’ mistuning z^* .

Conclusion

We have presented a general mistuning analysis and design package that combines two frameworks. The first is a mistuning analysis framework that exploits symmetry arguments and an eigenvalue/vector approximation technique to analyze any (low-order) mistuning model. The second is an aerodynamic model reduction framework that captures the content of a high-resolution CFD model with a small set of equations. Together, these frameworks have enabled the complete mistuning analysis of a turbomachinery model that includes sophisticated aerodynamics for the first time. In addition, the reduced-order aero-elastic model was sufficiently small to allow an application of robust analysis techniques to the mistuning problem. Hence we were able to rigorously prove that the intentional mistuning suggested by the symmetry/eigensystem approximation framework $z^* = 0.1(1, 1, \dots, 1, -1, -1, \dots, -1)$ improves the worst case forced response in a robust manner: any mistuning z within 1% of this mistuning value ($|z_j - z_j^*| \leq 0.01$ for all j) is guaranteed to have an acceptable forced response.

Acknowledgments

The research for this work was supported in part by a National Science Foundation Fellowship, a U.S. Air Force Office of Scientific Research Grant F49620-95-1-0409, and the Singapore Massachusetts Institute of Technology Alliance.

References

- Shapiro, B., “Symmetry Approach to Extension of Flutter Boundaries via Mistuning,” *Journal of Propulsion and Power*, Vol. 14, No. 3, May–June 1998, pp. 354–366.
- Shapiro, B., “Solving for Mistuned Forced Response by Symmetry,” *Journal of Propulsion and Power*, Vol. 15, No. 2, March–April 1999, pp. 310–325.
- Willcox, K., *Reduced-Order Aerodynamic Models for Aeroelastic Control of Turbomachines*, Ph.D. Dissertation, Dept. of Aeronautics and Astronautics, MIT, Feb. 2000.
- Sirovich, L., “Turbulence and the Dynamics of Coherent Structures. Part 1: Coherent Structures,” *Quarterly of Applied Mathematics*, Vol. 45, No. 3, Oct. 1987, pp. 561–571.
- Berkooz, G., Holmes, P., and Lumley, J., “The Proper Orthogonal Decomposition in the Analysis of Turbulent Flows,” *Annual Review of Fluid Mechanics*, Vol. 25, 1993, pp. 539–575.
- Dowell, E., and Hall, K., “Modeling of Fluid-Structure Interaction,” *Annual Review of Fluid Mechanics*, Vol. 33, 2001, pp. 445–90.
- Kim, T., “Frequency-Domain Karhunen-Loeve Method and Its Application to Linear Dynamic Systems,” *AIAA Journal*, Vol. 36, No. 11, 1998, pp. 2117–2123.
- Hall, K. C., Thomas, J. P., and Dowell, E. H., “Proper Orthogonal Decomposition Technique for Transonic Unsteady Aerodynamic Flows,” *AIAA Journal*, Vol. 38, No. 10, 2000, pp. 1853–62.
- Willcox, K., Paduano, J., Peraire, J., and Hall, K., “Low Order Aerodynamic Models for Aeroelastic Control of Turbomachines,” AIAA Paper 99-1467, April 1999.
- Dugundji, J., and Bundas, D., “Flutter and Forced Response of Mistuned Rotors Using Standing Wave Analysis,” *AIAA Journal*, Vol. 22, No. 11, 1984, pp. 1652–61.
- Al-Khayyal, F., Larsen, C., and Voorhis, T. V., “A Relaxation Method for Nonconvex Quadratically Constrained Quadratic Programs,” *Journal of Global Optimization*, Vol. 6, No. 3, 1995, pp. 215–230.
- Packard, A., and Doyle, J., “The Complex Structured Singular Value,” *Automatica*, Vol. 29, No. 1, 1993, pp. 71–109.